



## Biosorption potential of *Thapsia transtagana* stems for the removal of dyes: kinetics, equilibrium, and thermodynamics

A. Machrouhi<sup>a</sup>, M. Farnane<sup>a</sup>, A. Elhalil<sup>a</sup>, M. Abdennouri<sup>a</sup>, H. Tounsadi<sup>b</sup>, S. Qourzal<sup>c</sup>, N. Barka<sup>a,\*</sup>

<sup>a</sup>Laboratoire des Sciences des Matériaux, des Milieux et de la Modélisation (LS3M), FPK, Univ Hassan 1, B.P. 145, 25000 Khouribga, Morocco, Tel. +212 661 66 66 22; Fax: +212 523 49 03 54; email: barkanouredine@yahoo.fr (N. Barka), Tel. +21251039586; email: machrouhi.aicha90@gmail.com (A. Machrouhi), Tel. +21264832190; email: farnane.meryem@gmail.com (M. Farnane), Tel. +212678831928; email: elhalil.alaeddine@gmail.com (A. Elhalil), Tel. +212667669039; email: abdenmourimohamed@yahoo.fr (M. Abdennouri)

<sup>b</sup>Université Sidi Mohamed Ben Abdellah, Faculté des Sciences Dhar El Mahraz, Fès, Morocco, Tel. +21245208564; email: hananetounsadi@gmail.com (H. Tounsadi)

<sup>c</sup>Equipe de Catalyse et Environnement, Faculté des Sciences, Université Ibn Zohr, B.P. 8106 Cité Dakhla, Agadir, Maroc, Tel. 212662896006; email: samir\_qourzal@yahoo.fr (S. Qourzal)

Received 10 December 2017; Accepted 8 July 2018

### ABSTRACT

In this work, a low-cost and eco-friendly biosorbent developed from *Thapsia transtagana* stems (TTS) was investigated as an alternative to the current expensive methods for removing dyes from textile wastewater. Biosorption potential for the uptake of methylene blue (MB) and methyl violet (MV) was evaluated in batch mode under different condition. The experimental results show that biosorption yield increases with an increase in the biosorbent dosage. Maximum biosorption occurred at neutral to basic pH values. Kinetic data were properly fitted with the pseudo-first-order model instead of pseudo-second-order model. Equilibrium uptake was increased with an increase in the initial dye concentration in the range of 20–200 mg/L according to Langmuir isotherm model. The maximum monolayer biosorption capacities were 183.23 and 222.82 mg/g for MB and MV, respectively. The biosorption of the dyes was exothermic in nature ( $\Delta H^\circ = -21.07$  kJ/mol for MB and  $-16.85$  kJ/mol for MV). The reaction was accompanied by a decrease in entropy ( $\Delta S^\circ = -40.35$  J/K.mol for MB and  $-50.41$  J/K.mol for MV). The Gibbs energy ( $\Delta G^\circ$ ) increased from  $-4.91$  to  $-3.74$  kJ/mol and from  $-5.57$  to  $-4.22$  kJ/mol, respectively for MB and MV, when the temperature was increased from 25°C to 55°C. The surface of TTS has been thoroughly characterized by FTIR spectroscopy, scanning electron microscopy–energy-dispersive X-ray spectroscopy, Boehm titration, and point of zero charge.

**Keywords:** Biosorption; *Thapsia transtagana* stems; Textile dyes; Remediation

### 1. Introduction

Water pollution caused by organic pollutants has become a serious problem worldwide that threatens the balance of nature and the sustainable endurance of human beings [1]. Wastewaters from textile industries represent a serious

problem all over the world. They contain different types of synthetic dyes which are known to be a major source of environmental pollution, in terms of both the volume of dye discharged and the effluent composition [2–4]. Most of these dyes are toxic, mutagenic, and carcinogenic. Moreover, they are very stable to light, temperature, and microbial attack, making them recalcitrant compounds. From an

\* Corresponding author.

environmental point of view, the removal of synthetic dyes is of great concern.

Nowadays, many treatment processes like coagulation, flocculation, ion exchange, membrane separation, reverse osmosis, oxidation, etc. are available for the removal of dyes from aqueous solution. Major drawbacks of these methods include handling and disposal problems, high cost, technical constraints, etc. However, adsorption is preferred for the removal of these pollutants due to easy handling and removal performance. On the other hand, the economy and efficacy of the adsorption process are limited by the physico-chemical characteristics and the cost of the adsorbent [5–9].

Various biomasses have been tested to reduce dye concentrations from aqueous solutions as potential biosorbents such as carob shells [10], tomato waste [11], mango seed kernel [12], jackfruit leaf [13], *Diplotaxis harra* and *Glebionis coronaria* L. [14], sugar beet pulp [15], *Bacillus cereus* [16], *Ziziphus lotus* fruit peels, and avocado kernels seeds [17]. However, the adsorption capacities of the abovementioned adsorbents are not very high. In order to improve the efficiency of the adsorption processes, it is necessary to develop cheaper and easily available adsorbents with high-adsorption capacities.

The focus of this study was to assess the potentiality of *Thapsia transtagana* stems (TTS) for the removal of synthetic dyes from aqueous solutions. This plant is plentiful, easily available, and non-toxic. We chose, in this study, methylene blue (MB) as a model compound because of its strong adsorption study on solids and its use in characterizing adsorptive materials. Methyl violet (MV) dye was also used as a model compound of textile dyes.

Biosorption experiments were carried out as function of contact time, biosorbent dosage, initial concentration of dyes, temperature, and solution pH. Biosorption kinetic data were fitted to the pseudo-first-order and the pseudo-second-order kinetic models. Equilibrium isotherms were modeled by Langmuir and Freundlich models. The surface properties of biomass were characterized by FTIR, scanning electron microscopy–energy-dispersive X-ray spectroscopy (SEM–EDX), and the pH of point of zero charge (pHpzc). The functional groups were also determined by Boehm titration.

## 2. Experimental

### 2.1. Materials

All chemicals used in this study were of analytical grade. Cd (NO<sub>3</sub>)<sub>2</sub>·4H<sub>2</sub>O (98%), Co (NO<sub>3</sub>)<sub>2</sub>·6H<sub>2</sub>O (98%), NaCl (99.5%), HCl (37%), Na<sub>2</sub>CO<sub>3</sub>, NaHCO<sub>3</sub>, and MV 2B dye were obtained from Sigma-Aldrich (Germany). HNO<sub>3</sub> (65%) was from Scharlau (Spain), NaOH (98%) from Merck (Germany), and MB dye was from Panreac (Spain). The characteristics and chemical structure of the dyes are listed in Table 1.

### 2.2. Preparation and characterization of the biosorbent

TTS used in this study was collected from the region of Oued Zem in Morocco. It was first cleaned, dried in sunlight, cut into small pieces, and then powdered to a particle sizes lesser than 125 μm using a domestic mixer. The powdered biosorbent was stored in hermetic glass bottle for further use. FTIR transmittance spectra of the biosorbent were recorded in the region of 4,000–400 cm<sup>-1</sup> by using a Scottech-SP-1

spectrophotometer. Samples were prepared as KBr pellets under high pressure. The surface morphology was observed by SEM using an FEI Quanta 200 model. The pHpzc was determined according to the method described by Noh and Schwarz [18]. The pH of NaCl aqueous solution (50 mL at 0.01 mol/L) was adjusted to successive initial values in the range of 2–12 by addition of HNO<sub>3</sub> and/or NaOH. Moreover, 0.05 g of each biosorbent was added in the solution and stirred for 6 h. The final pH was measured and plotted vs. the initial pH. The pHpzc was determined at the value for which pH<sub>final</sub> = pH<sub>initial</sub>. Basic and oxygenated acidic surface groups were quantified by Boehm titrations [19]. About 0.1 g of each sample was mixed with 50 mL of 0.01 M aqueous reactant solution (NaOH, Na<sub>2</sub>CO<sub>3</sub>, NaHCO<sub>3</sub>, or HCl). The mixtures were stirred at 500 rpm for 24 h at room temperature. Then, the suspensions were filtrated by a 0.2 μm membrane filter. To determine the content of oxygenated groups, back titrations of the filtrate (10 mL) were achieved with standard 0.01 M HCl solution. Basic group's content was also determined by back titration of the filtrate with 0.01 M NaOH solution.

### 2.3. Biosorption studies

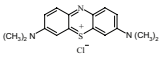
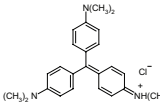
Batch equilibrium experiments were performed to determine the efficiency of TTS for the removal of MB and MV from aqueous solution under various process conditions. The effect of initial solution pH on the removal efficiency was analyzed over the pH range 2–11. The pH was adjusted using 0.1 N NaOH and/or 0.1 N HNO<sub>3</sub> solutions. The effect of *T. transtagana* dosage was investigated in the range of 0.1–6 g/L. Kinetic was carried out by varying the contact time from 2 to 180 min. Experiments were done by agitating 250 mL of dyes solutions of 50 mg/L with 0.2 g/L of biosorbent. Biosorption equilibrium was established for different dyes initial concentrations between 20 and 200 mg/L. The effect of solution temperature was tested in the range of 25°C–55°C.

After each biosorption experiment was completed, the solid phase was separated from the liquid phase by centrifugation at 3,000 rpm for 10 min. Samples were diluted by distilled water, and the residual concentrations were determined from UV–Vis spectrophotometer.

The adsorbed amounts and the removal efficiency were calculated by the following equations:

$$q = \frac{(C_0 - C)}{R} \quad (1)$$

Table 1  
Molecular structure and physical characteristics and of MB and MV

Name	Molecular structure	M <sub>w</sub> (g/mol)	λ <sub>max</sub> (nm)
Methylene blue (basic blue 9)		319.85	661
Methyl violet 2B (basic violet 1)		393.95	584

$$\% \text{ Removal} = \frac{(C_0 - C)}{C_0} \times 100 \quad (2)$$

where  $q$  is the adsorbed amounts (mg/g),  $C_0$  is the initial dye concentration (mg/L),  $C$  is the dye concentration after biosorption, and  $R$  is the mass biosorbent per liter of solution (g/L).

#### 2.4. Adsorbent regeneration

Batch process was employed for MB desorption and regeneration. The TTS was loaded with 1L MB solution of 50 mg/L initial concentration at initial pH and contact time 3 h. After saturation, the suspension was filtered, and the residual solid was contacted with distilled water or various solutions of  $H_2SO_4$ ,  $HNO_3$ , NaOH, and NaCl of 0.1N each as the desorbing solution at the same operating conditions adopted in adsorption. Regeneration studies were conducted by using the same adsorbent. The percentage of MB desorbed was calculated by the following equation:

$$\% \text{ Desorption} = \frac{100 \times C_d}{q_e \times R} \quad (3)$$

where  $C_d$  (mg/L) is the concentration of MB desorbed,  $q_e$  (mg/g) is the adsorption capacity of the adsorbent, and  $R$  is the weight ratio of the TTS used in desorption.

### 3. Results and discussion

#### 3.1. Characterization

##### 3.1.1. FTIR analysis

FTIR spectroscopy in the range of 400–4,000  $cm^{-1}$  was employed to obtain information on the nature of functional groups at the surface of the biosorbent. The spectrum presented in Fig. 1 shows broad, strong, and superimposed bands around 3,600–3,200  $cm^{-1}$  which may be due to overlapping of the stretching vibration of hydrogen-bonded of the hydroxyl group linked in cellulose, lignin, adsorbed

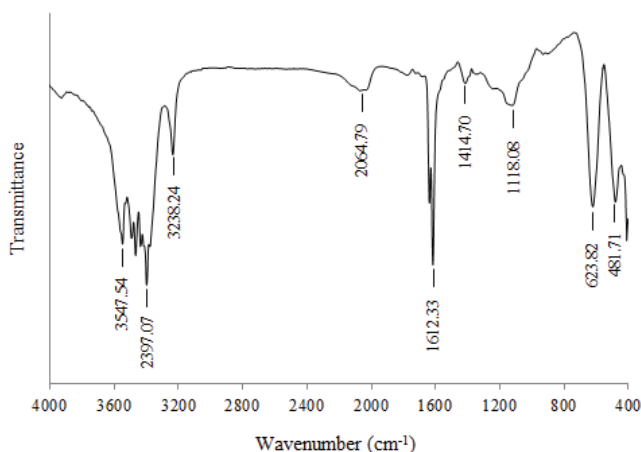


Fig. 1. FTIR spectrum of TTS biosorbent.

water, and N–H stretching [20]. A weak absorption peaks at 1,757  $cm^{-1}$  is attributed to stretching of carboxyl groups. The bands at 1,635  $cm^{-1}$  is indicative of OH bending vibrations. The strong absorption band at 1,614  $cm^{-1}$  is characteristic of C=O stretching vibrations of ketones, aldehydes, lactones, or carboxyl groups [10]. The band at 1,414  $cm^{-1}$  is corresponding of C–O stretching. The band at 1,360  $cm^{-1}$  assigned to C–N groups on the biomass surface. The absorption peaks around 1,160 and 1,060  $cm^{-1}$  are indicative of P=O and P–OH stretching vibrations. Peaks in the region of wavenumbers lower than 800  $cm^{-1}$  could be attributed to N-containing bioligands.

##### 3.1.2. Boehm titration and pH<sub>pzc</sub>

Surface functional groups play an important role in sorption processes. These functional groups are principally divided as acidic or basic groups, which affect the surface charge of the biosorbent and consequently the biosorption efficiency [21]. Boehm titration was used to quantify the surface functional groups present on TTS biosorbent. The obtained result is illustrated in Table 2. From the table, it can be seen that the biosorbent surfaces are constituted mainly of acidic groups which are due to presence of carboxylic, phenolic, and lactonic groups and a less quantity of basic groups. Generally, biosorbent with greater surface acid groups have a higher cation exchange property. These results suggest greater sorption performance for selected dyes. The pH<sub>pzc</sub> of the biosorbent was found to be 6.5 (Fig. 2). This value is in agreement with Boehm titration result, which shows a dominance of acidic groups at the surface of the biosorbents.

##### 3.1.3. SEM–EDX analysis

The surface of TTS was analyzed by SEM as shown in Fig. 3. The figure indicates that TTS has rough surface with

Table 2  
Chemical groups on the surface of TTS biosorbent

Functional groups (meq/g)				
Carboxylic	Lactonic	Phenolic	Total acid	Total basic
0.484	0.494	0.516	1.494	0.409

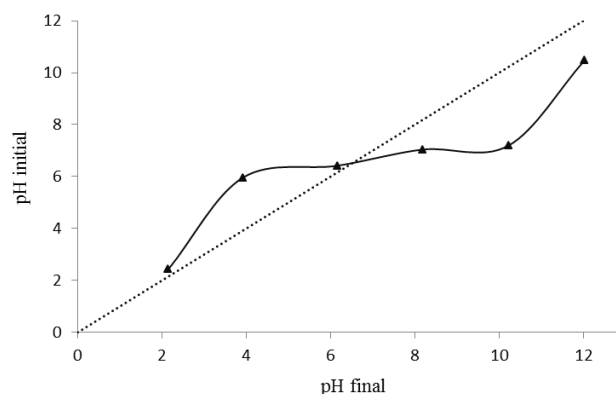


Fig. 2. Determination of the point of zero charge (pHpzc) of TTS.

irregular structure morphology and pores of different size and different shape. This kind of morphology can favor the biosorption of dyes on different parts of the biosorbent. The chemical composition was identified by the EDX analysis. The EDX spectrum with chemical compositions for TTS is given in Fig. 4. The EDX spectrum revealed mainly the presence of carbon (63.27%) and oxygen (31.45%) associated with some minerals such as potassium, nitrogen, and calcium.

### 3.2. Biosorption performance

#### 3.2.1. Effect of pH on the removal of dyes

The pH of aqueous solutions is an important factor that controls the surface chemistry of biosorbent and ionic state of dye molecules. Changes observed in the biosorption of MB and MV by TTS as a function of solution pH are presented in Fig. 5. The figure indicates that the biosorption was weak in acidic medium and increases with the increase in solution pH. Both the dyes give the same behavior with solution pH, which suggest that surface of biosorbent was the main factor controlling these changes. The pHPzc of the biosorbent was found to be 6.5 indicating that for pH values higher than 6.5, the surface of the biosorbent particles becomes negatively charged, and the opposite for pH less than 6.5. Consequently, the adsorption of dyes at acidic pH is disfavored by repulsive forces existing between functional groups of the dye

molecules and the positively charged surface of the biosorbents, which is predominant in this range of pH [22,23]. The optimal pH for high sorption of MB and MV were achieved at pH = 5.00 and 5.71, respectively.

#### 3.2.2. Effect of biosorbents dosage

Fig. 6 illustrates the effect of biosorbent dosage on the biosorption of MB and MV. This figure indicates that the biosorption yield increased from 36.58% to 87.61% and from 55.06% to 89.93%, respectively for MB and MV, when the biosorbent dosage was increased from 0.1 to 6 g/L. This can be expected because the higher the dose of biosorbent in the solution, the greater is the availability of exchangeable sites for the pollutants [24]. Even though the removal efficiency increased with adsorbent dosage, the biosorption capacity decreased with increase in biosorbent dosage. This is because the amount of dye molecules in contact with unit weight of biosorbent decreases with increase in biosorbent dosage. From a practical viewpoint, the optimum dosage of 0.2 g/L was chosen in further experiments.

#### 3.2.3. Biosorption kinetics

Kinetics of biosorption is desirable as it provides information about the dynamic of the reaction in terms of order and of the rate constant, which is important for efficiency of

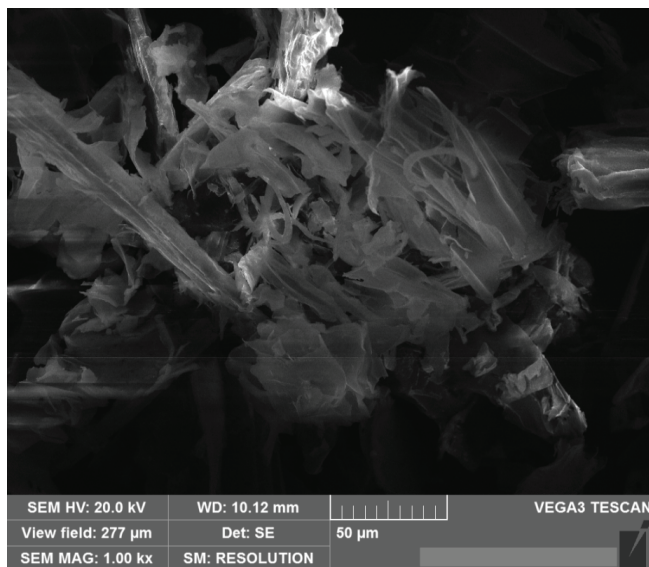


Fig. 3. SEM image of TTS.

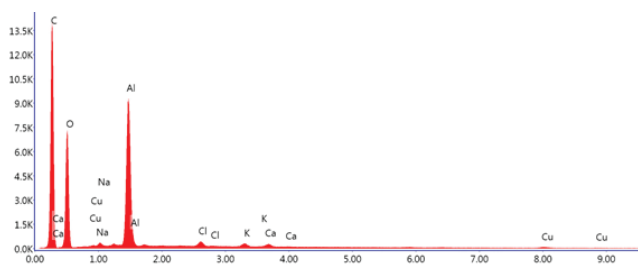


Fig. 4. Energy-dispersive X-ray (EDX) analysis of TTS.

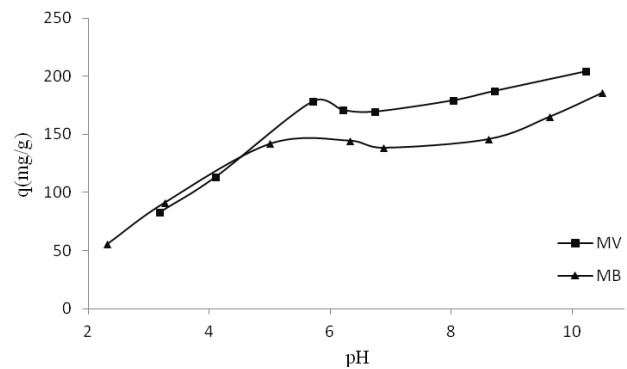


Fig. 5. Effect of pH on the biosorption of MB and MV onto TTS:  $C_0 = 50$  mg/L, contact time = 120 min,  $R = 0.2$  g/L, and  $T = 25^\circ\text{C}$ .

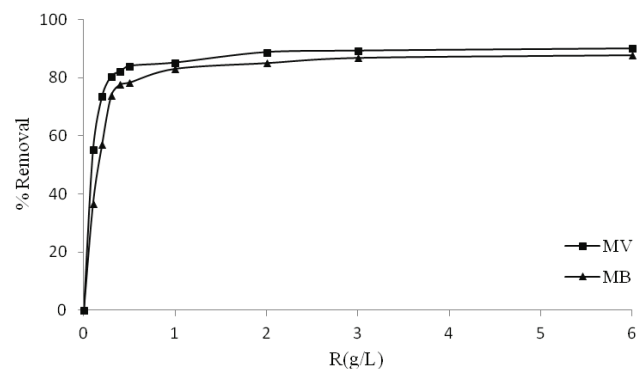


Fig. 6. Effect of biosorbent dosage on the biosorption of MB and MV onto TTS:  $C_0 = 50$  mg/L, contact time = 120 min, initial pH, and  $T = 25^\circ\text{C}$ .



the process. Fig. 7 shows the variation of biosorbed amounts of dyes vs. contact time. The figure shows that the biosorption was found to be rapid at the first period of the process, and then the rate of biosorption becomes slower and then stagnates with the increase in contact time. The equilibrium times was found to be 60 min for the both dyes. Biosorption kinetics data were analyzed using two kinetic models, pseudo-first-order model [25] and pseudo-second-order model [26].

The first-order rate expression of Lagergren based on solid capacity is generally expressed as follows:

$$q = q_e(1 - e^{-k_1 t}) \quad (4)$$

where  $q_e$  and  $q$  (both in mg/g) are, respectively, the amounts of dye biosorbed at equilibrium and at any time  $t$  (min) and  $k_1$  (1/min) is the rate constant of biosorption.

The pseudo-second-order model can be expressed as follows:

$$q = \frac{k_2 q_e^2 t}{1 + k_2 q_e t} \quad (5)$$

where  $k_2$  (g/mg min) is the rate constant of pseudo-second-order biosorption.

Parameters of the pseudo-first-order and pseudo-second-order models were estimated with the aid of the nonlinear regression. The obtained data and the correlation coefficients,  $r^2$ , are given in Table 3. The table shows that the

calculated equilibrium values ( $q_{cal}$ ) from pseudo-first-order model were close to the experimental values ( $q_{exp}$ ) than the others calculated from the pseudo-second-order kinetic model. Moreover, the correlation coefficients were closer to 1 in the case of pseudo-first-order than of pseudo-second-order model. This result suggests that the biosorption of MB and MV onto TTS could be better described by the pseudo-first-order model instead of pseudo-second-order kinetic model. Therefore, these observations are in agreement with the experimental results presented in Fig. 7, which indicates that the biosorption of MB and MV from aqueous solution onto TTS biomass occurs through two consecutive stages. During the first stage, which is a fast one, the biosorption processes take place at the surface and are probably determined by the chemical interactions that bind the cationic dyes on the biomass surface. The second stage, which occurs more slowly, involves the diffusion of cationic dyes inside of biosorbent structure [27].

### 3.2.4. Biosorption isotherms

Biosorption isotherms are another important tool that helps understanding the mechanism of the biosorption process. Also, the equilibrium biosorption studies determine the capacity of the biosorbent, which can be described by a biosorption isotherm, characterized by certain constants whose values inform the surface properties, heterogeneity, biosorption intensity, and affinity of the particular adsorbent [28]. Moreover, it gives the information about the distribution of the solute between the liquid and solid phases at various equilibrium concentrations. The biosorption isotherms are

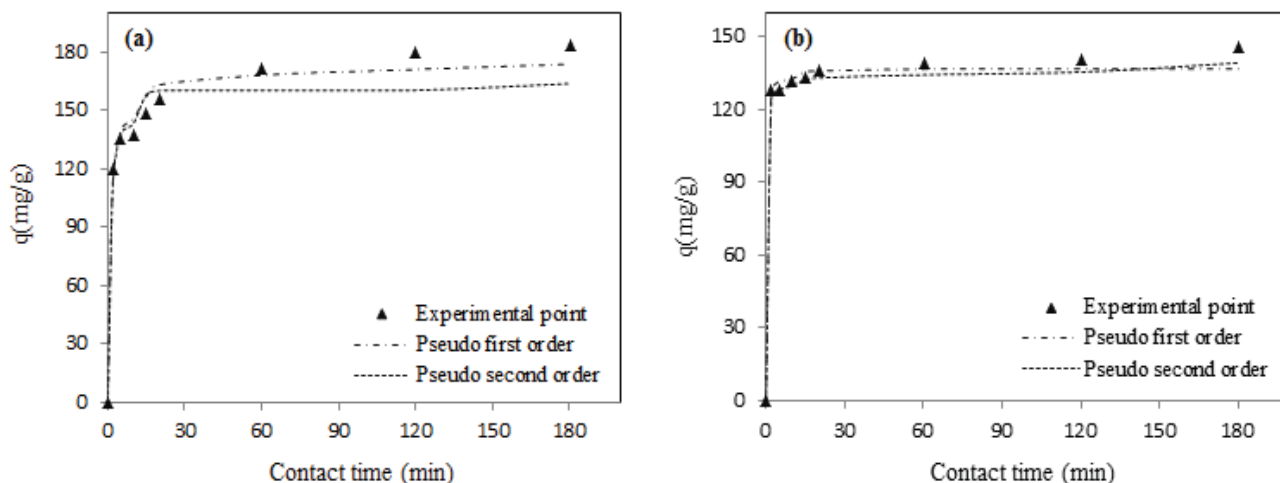


Fig. 7. Kinetics of (a) MV and (b) MB biosorption by TTS:  $C_0 = 50$  mg/L,  $R = 0.2$  g/L, initial pH, and  $T = 25^\circ\text{C}$ .

Table 3

Pseudo-first-order and pseudo-second-order kinetic parameters for the biosorption of MB and MV

Dye	$q_{exp}$ (mg/g)	Pseudo first order			Pseudo second order		
		$q_{cal}$ (mg/g)	$k$ (1/min)	$r^2$	$q_{cal}$ (mg/g)	$k$ (g/mg min)	$r^2$
MB	140.84	136.75	1.365	0.985	139.314	0.030	0.981
MV	179.80	173.55	0.005	0.971	163.614	0.554	0.925

illustrated in Fig. 8. The figure indicates that dyes removal is highly concentration dependent. The increase in biosorption capacity with concentration is probably due to a high driving force for mass transfer. In fact, high concentration in solution implicates high dye molecules fixed at the surface of the biosorbent. Equilibrium data obtained were analyzed using Langmuir and Freundlich isotherm models.

The Langmuir [29] isotherm assumes that the numbers of surface biosorption sites are fixed, biosorption behavior is independent of surface coverage, and all adsorption sites are represented by similar types of functional groups. The Langmuir model is the most frequently used in many sorption processes to evaluate the maximum sorption capacity. The linear form of Langmuir isotherm is represented as follows:

$$q_e = \frac{q_m K_L C_e}{1 + K_L C_e} \tag{6}$$

where  $q_m$  (mg/g) is the maximum monolayer biosorption capacity,  $K_L$  (L/mg) is the Langmuir equilibrium constant related to the biosorption affinity, and  $C_e$  is the equilibrium concentration.

The Freundlich isotherm is an empirical model of heterogeneous surface sorption with non-uniform distribution of heat sorption and affinities [30]. The form of the Freundlich equation can be stated as follows:

$$q_e = K_f C_e^{1/n} \tag{7}$$

where  $K_f$  ( $\text{mg}^{1-1/n} \text{g}^{-1} \text{L}^{1/n}$ ) is the Freundlich constant and  $n$  is the heterogeneity factor. The  $K_f$  value is related to the biosorption capacity; while  $1/n$  value is related to the biosorption intensity.

The calculated parameters for Langmuir and Freundlich models are reported in Table 4. From the table, it can be seen that Langmuir model indicates higher values of correlation coefficients than Freundlich model. These results indicated that the biosorption of dyes was best fitted by the Langmuir isotherm model. The maximum monolayer biosorption capacities were found to be 183.23 and 222.82 mg/g, respectively for MB and MV. These values were compared with those of similar biosorbents reported in the literature as given in Table 5. It can be observed that the results of this study were found to be higher than those of the majority of the related biosorbents given in this table. Therefore, this adsorption behavior is probably determined by the relaxed structure of the adsorbent. The existence of physical bonds between functional groups proved by FTIR spectra (Fig. 1) prevents the penetration of cationic dyes inside of adsorbent material particles, and in consequence, the adsorption process occurs only at TTS surface, being well described by Langmuir model [31].

### 3.2.5. Effect of temperature and thermodynamic parameters

The biosorption of the dyes was studied at various temperatures from 25°C to 55°C as shown in Fig. 9. A decrease in the removal efficiency was observed with an increase in solution temperature. Generally, the temperature has two major effects on the biosorption process. Increasing the temperature is known to increase the rate of the diffusion of molecules

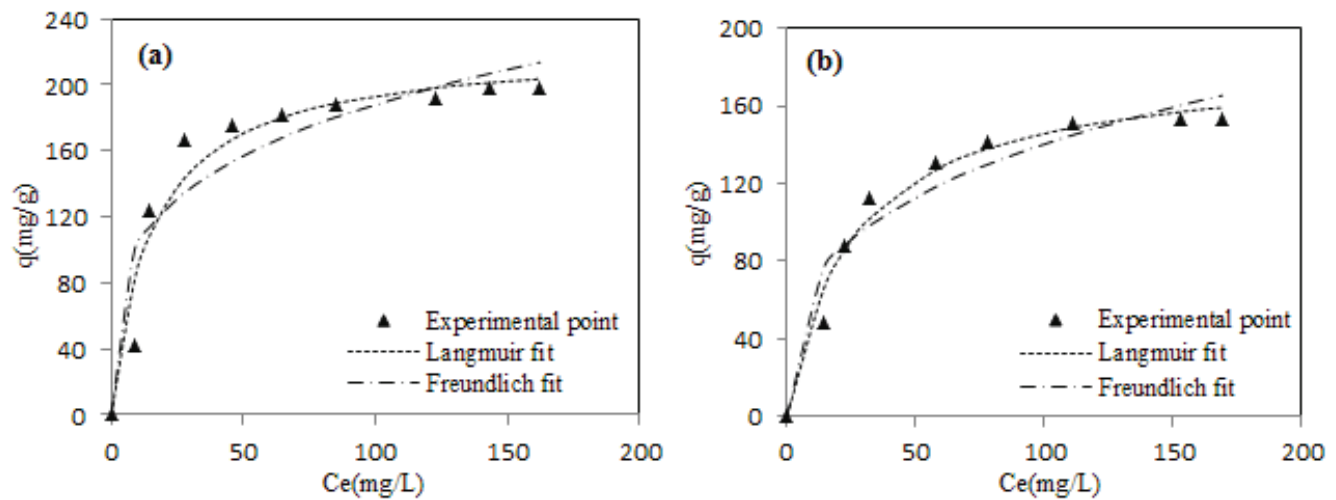


Fig. 8. Biosorption isotherms of (a) MV and (b) MB onto TTS.

Table 4  
Isotherm parameters and correlation coefficients calculated for the biosorption of MB and MV onto TTS

Dye	Langmuir			Freundlich		
	$q_m$ (mg/g)	$K_L$ (L/mg)	$r^2$	$K_f$ ( $\text{mg}^{1-1/n} \text{g}^{-1} \text{L}^{1/n}$ )	$n$	$r^2$
MB	183.23	0.039	0.980	33.33	3.20	0.937
MV	222.82	0.065	0.946	56.45	3.82	0.878

across the external boundary layer and the internal pores of the biosorbent particles, owing to the decrease in the viscosity of the solution. In addition, changing temperature will change the equilibrium capacity of the biosorbent for a particular adsorbate [44]. From these results, thermodynamic parameters including the change in free energy ( $\Delta G^\circ$ ), enthalpy ( $\Delta H^\circ$ ), and entropy ( $\Delta S^\circ$ ) were used to describe thermodynamic behavior of the biosorption of the dyes. These parameters were calculated by considering the following reversible process:

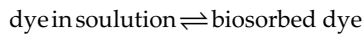


Table 5  
Comparison of biosorption capacity of TTS for MB and MV with different related biosorbents

Biosorbent	$q_m$ (mg/g)		References
	MV	MB	
Mansonia sawdust	16.11	28.89	[32]
Peach gum	277	–	[33]
Banana pith	12	–	[34]
Peanut straw char	256.4	–	[35]
Soybean straw char	178.6	–	[35]
Rice hull char	123.5	–	[35]
Bagasse fly ash	26.25	–	[36]
Beetroot seeds	–	61.11	[37]
Crosslinked amphoteric starch	333.33	–	[38]
Sunflower seed hull	92.59	–	[39]
Sugarcane dust	50.40	–	[40]
Breadnut core	–	369.00	[41]
<i>Ziziphus lotus</i> fruits peel	–	66.04	[17]
Avocado kernel seeds	–	59.07	[17]
<i>Casuarina equisetifolia</i> needle	–	77.60	[42]
Garlic peel	–	82.6	[43]
<i>Diplotaxis harra</i>	–	185.59	[14]
<i>Glebionis coronaria</i> L.	–	258.76	[14]
<i>Thapsia transtaganana</i> stems	222.82	183.23	This study

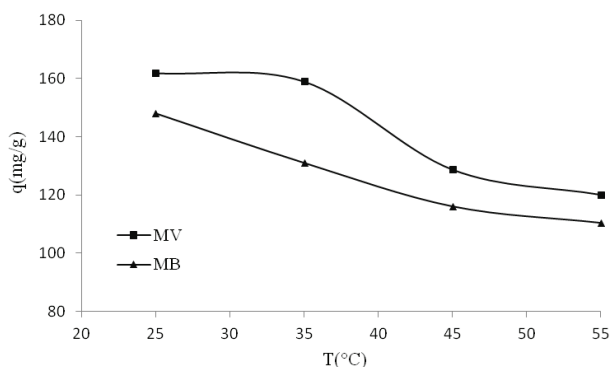


Fig. 9. Effect of temperature on the biosorption of MB and MV onto TTS:  $C_0 = 50$  mg/L, contact time = 120 min, initial pH, and  $R = 0.2$  g/L.

For such equilibrium reactions,  $K_D$ , the distribution constant, can be expressed as follows:

$$K_D = \frac{q_e}{C_e} \quad (8)$$

The Gibbs free energy is as follows:

$$\Delta G^\circ = -RT \ln(K_D) \quad (9)$$

where  $R$  is the universal gas constant (8.314 J mol/K) and  $T$  is solution temperature in K.

The enthalpy ( $\Delta H^\circ$ ) and entropy ( $\Delta S^\circ$ ) of biosorption were estimated from the slope and intercept of the plot of  $\ln K_D$  vs.  $1/T$  yields, respectively.

$$\ln K_D = -\frac{\Delta G^\circ}{RT} = -\frac{\Delta H^\circ}{RT} + \frac{\Delta S^\circ}{R} \quad (10)$$

The thermodynamic parameters calculated from the values of the slopes and the intercepts are reported in Table 6. The negative values of  $\Delta G^\circ$  at different temperatures indicate that the biosorption is thermodynamically feasible and is a spontaneous process. The increase in  $\Delta G^\circ$  values with increase in temperature shows a decrease in feasibility of biosorption at higher temperatures. The enthalpy of biosorption ( $\Delta H^\circ$ ) was found to be  $-16.85$  kJ/mol for MB and  $-21.07$  kJ/mol for MV. The negative  $\Delta H^\circ$  is indicator of exothermic nature of the biosorption and also its magnitude gives information on the type of biosorption, which can be either physical or chemical. The negative value of  $\Delta S^\circ$  for the corresponding temperature interval indicated decreased randomness at the solid–solution interface with the loading of species onto the surface of TTS. It also suggested the probability of a favorable biosorption process.

### 3.3. Desorption and regeneration study

The recycling of adsorbate and successive regeneration and reuse of adsorbent are important issues step in order to check the economic feasibility of adsorption process. Hence, this study was dedicated to investigate the feasibility of

Table 6  
Thermodynamic parameters calculated for the biosorption of MV and MB by TTS

	$T$ (K)	$K_D$	$\Delta G^\circ$ (kJ/mol)	$\Delta H^\circ$ (kJ/mol)	$\Delta S^\circ$ (J/K.mol)
Methyl violet 2B	298	9.480	-5.57	-21.07	-50.41
	308	9.006	-5.63		
	318	5.428	-4.47		
Methylene blue	328	4.718	-4.23	-16.85	-40.35
	298	7.253	-4.91		
	308	5.502	-4.38		
	318	4.329	-3.89		
	328	3.950	-3.74		

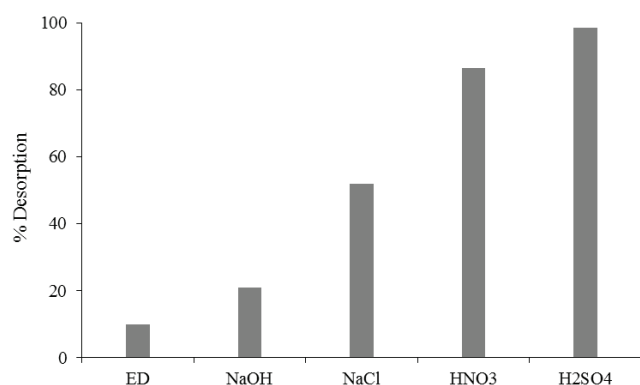


Fig. 10. Desorption of MB from TTS by various eluents.

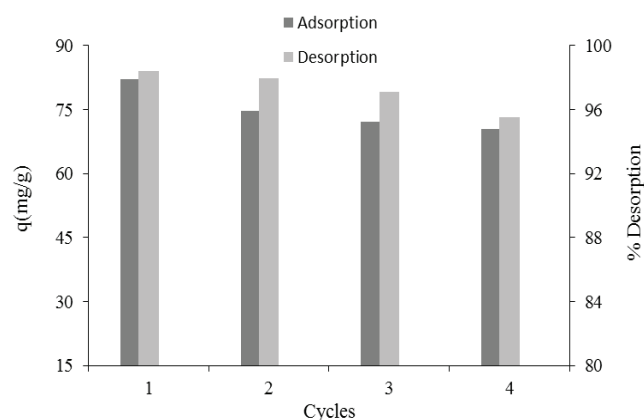


Fig. 11. Removal efficiency of TTS in four successive cycles of adsorption–desorption compared with the original adsorption capacity.

using chemical regeneration for MB elution. Results of MB desorption using deionized water, NaOH, NaCl, HNO<sub>3</sub>, and H<sub>2</sub>SO<sub>4</sub>/HCl treatments are shown in Fig. 10. The figure indicates that MB elution by using 0.1 N H<sub>2</sub>SO<sub>4</sub> was optimum (98.61%) followed by HNO<sub>3</sub> (0.1 N), NaCl (0.1 N), NaOH (0.1 N), and deionized water. Thereafter, four cycles of adsorption–desorption were performed using H<sub>2</sub>SO<sub>4</sub> solution (0.1 N). The results given in Fig. 11 showed that the adsorption capacity does not strongly decrease after four cycles of desorption–adsorption compared with the original adsorption capacity. This decrease in adsorption capacity might be caused by the decomposition or damage caused by acidic solution to certain adsorption sites or functional groups present over TTS surface [45].

#### 4. Conclusion

This work evaluated the potential of TTS for the removal of MB and MV from aqueous solutions. It was found that the biosorbent has rough surface with irregular structure morphology and pores of different size and different shape. The surface of the particles was constituted mainly of acidic groups. Biosorption yield was affected by contact time, solution pH, biosorbent dosage, and initial concentration. The biosorption yield increases with the increase in biosorbent

dosage. An optimum of 0.2 g/L was obtained. The optimum sorption capacity was obtained at neutral pH medium. Kinetics and equilibrium data fitted well the first-order kinetic model and the Langmuir model, respectively, with good values of the determination coefficient. The biosorption was thermodynamically feasible and is a spontaneous process. Finally, this study showed that low-cost, locally sourced, and ubiquitous TTS biosorbent have good potential for the removal of textile dyes from wastewaters.

#### References

- [1] H. Kyung, J. Lee, W. Choi, Simultaneous and synergistic conversion of dyes and heavy metal ions in aqueous TiO<sub>2</sub> suspensions under visible-light illumination, *Environ. Sci. Technol.*, 39 (2005) 2376–2382.
- [2] M.A. Rauf, S.M. Qadri, S. Ashraf, K.M. Al-Mansoori, Adsorption studies of toluidine blue from aqueous solutions onto gypsum, *Chem. Eng. J.*, 150 (2009) 90–95.
- [3] T. Robinson, G. McMullan, R. Marchant, P. Nigam, Remediation of dyes in textile effluent: a critical review on current treatment technologies with a proposed alternative, *Bioresour. Technol.*, 77 (2004) 247–255.
- [4] F.Z. Mahjoubi, A. Khalidi, M. Abdennouri, N. Barka, M-Al-SO<sub>4</sub> layered double hydroxides (M=Zn, Mg or Ni): synthesis, characterization and textile dyes removal efficiency, *Desal. Wat. Treat.*, 57 (2016) 21564–21576.
- [5] N. Chiron, R. Guilet, E. Deydier, Adsorption of Cu(II) and Pb(II) onto a grafted silica: isotherms and kinetic models, *Water Res.*, 37 (2003) 3079–3086.
- [6] L. Semerjian, Equilibrium and kinetics of cadmium adsorption from aqueous solutions using untreated *Pinus halepensis* sawdust, *J. Hazard. Mater.*, 173 (2010) 236–242.
- [7] M. Ozacar, A. Sengil, Adsorption of reactive dyes on calcined alunite from aqueous solutions, *J. Hazard. Mater.*, 98 (2003) 221–224.
- [8] S. Debnath, U.C. Ghosh, Nanostructured hydrous titanium(IV) oxide: synthesis, characterization and Ni(II) adsorption behavior, *Chem. Eng. J.*, 152 (2009) 480–491.
- [9] K. Shi, X. Wang, Z. Guo, S. Wang, W. Wu, Se(IV) sorption on TiO<sub>2</sub>: sorption kinetics and surface complexation modeling, *Colloids Surf., A*, 349 (2009) 90–95.
- [10] M. Farnane, H. Tounsadi, R. Elmoubarki, F.Z. Mahjoubi, A. Elhalil, S. Saqrane, M. Abdennouri, S. Qourzal, N. Barka, Alkaline treated carob shells as sustainable biosorbent for clean recovery of heavy metals: kinetics, equilibrium, ions interference and process optimization, *Ecol. Eng.*, 101 (2017) 9–20.
- [11] A.Ş. Yargıç, R.Z. Yarbay Şahin, N. Özbay, E. Önal, Assessment of toxic copper(II) biosorption from aqueous solution by chemically-treated tomato waste, *J. Cleaner Prod.*, 88 (2015) 152–159.
- [12] P. Senthil Kumar, M. Palaniyappan, M. Priyadarshini, A.M. Vignesh, A. Thanjiappan, P. Sebastina Anne Fernando, R. Tanvir Ahmed, R. Srinath, Adsorption of basic dye onto raw and surface-modified agricultural waste, *Environ. Prog. Sustainable Energy*, 33 (2014) 87–98.
- [13] A.K. Ojha, V.K. Bulasara, Adsorption characteristics of jackfruit leaf powder for the removal of Amido black 10B dye, *Environ. Prog. Sustainable Energy*, 34 (2015) 461–470.
- [14] H. Tounsadi, A. Khalidi, M. Abdennouri, N. Barka, Potential capability of natural biosorbents: *Diplotaxis harra* and *Glebionis coronaria* L. on the removal efficiency of dyes from aqueous solutions, *Desal. Wat. Treat.*, 57 (2016) 16633–16642.
- [15] S.T. Akar, D. Yilmazer, S. Celik, Y.Y. Balk, T. Akar, On the utilization of a lignocellulosic waste as an excellent dye remover: modification, characterization and mechanism analysis, *Chem. Eng. J.*, 229 (2013) 257–266.
- [16] P. Arivalagan, D. Singaraj, V. Haridass, T. Kaliannan, Removal of cadmium from aqueous solution by batch studies using *Bacillus cereus*, *Ecol. Eng.*, 71 (2014) 728–735.



- [17] A. Machrouhi, A. Elhalil, M. Farnane, F.Z. Mahjoubi, H. Tounsadi, M. Sadiq, M. Abdennouri, N. Barka, Adsorption behavior of methylene blue onto powdered *Ziziphus lotus* fruit peels and avocado kernels seeds, *J. Appl. Surf. Interface*, 1 (2017) 49–56.
- [18] J.S. Noh, J.A. Schwarz, Estimation of the point of zero charge of simple oxides by mass titration, *J. Colloid Interface Sci.*, 130 (1989) 157–164.
- [19] H.P. Boehm, Surface oxides on carbon and their analysis: a critical assessment, *Carbon*, 40 (2002) 145–149.
- [20] M.R.H. Mas Haris, K. Sathasivam, The removal of methyl red from aqueous solutions using banana pseudostem fibers, *Am. J. Appl. Sci.*, 6 (2009) 1690–1700.
- [21] S. Deng, R. Bai, Removal of trivalent and hexavalent chromium with aminated polyacrylonitrile fibers: performance and mechanisms, *Water Res.*, 38 (2004) 2424–2432.
- [22] R.K. Xu, S.-C. Xiao, J.-H. Yuan, A.-Z. Zhao, Adsorption of methyl violet from aqueous solutions by the biochars derived from crop residues, *Bioresour. Technol.*, 102 (2011) 10293–10298.
- [23] X. Han, X. Niu, X. Ma, Adsorption characteristics of methylene blue on poplar leaf in batch mode: equilibrium, kinetics and thermodynamics, *Korean J. Chem. Eng.*, 29 (2012) 494–502.
- [24] M. Farnane, A. Elhalil, A. Machrouhi, F.Z. Mahjoubi, M. Sadiq, M. Abdennouri, S. Qourzal, H. Tounsadi, N. Barka, Enhanced adsorptive removal of cationic dyes from aqueous solution by chemically treated carob shells, *Desal. Wat. Treat.*, 100 (2017) 204–213.
- [25] S. Lagergren, About the theory of so-called adsorption of soluble substance, *Kungliga Svenska Vetenskapsakademiens Handlingar*, 24 (1898) 1–39.
- [26] Y.S. Ho, G. McKay, Pseudo-second order model for sorption processes, *Process Biochem.*, 34 (1999) 451–465.
- [27] L. (Negrilă) Nemeș, L. Bulgariu, Optimization of process parameters for heavy metals biosorption onto mustard waste biomass, *Open Chem.*, 14 (2016) 175–187.
- [28] R. Malik, S. Dahiya, S. Iata, An experimental and quantum chemical study of removal of utmostly quantified heavy metals in wastewater using coconut husk: a novel approach to mechanism, *Inter. J. Biol. Macromol.*, 98 (2017) 139–149.
- [29] I. Langmuir, The constitution and fundamental properties of solids and liquids. Part I. Solids, *J. Am. Chem. Soc.*, 38 (1916) 2221–2295.
- [30] H. Freundlich, W. Heller, The Adsorption of cis- and trans-Azobenzene, *J. Am. Chem. Soc.*, 61 (1939) 2228–2230.
- [31] G. Nacu, D. Bulgariu, M.C. Popescu, M. Harja, D.T. Juravle, L. Bulgariu, Removal of Zn(II) ions from aqueous media on thermal activated sawdust, *Desal. Wat. Treat.*, 57 (2016) 21904–21915.
- [32] A.E. Ofomaja, Kinetic study and sorption mechanism of methylene blue and methyl violet onto mansonia (*Mansonia altissima*) wood sawdust, *Chem. Eng. J.*, 143 (2008) 85–95.
- [33] Li. Zhou, J. Huang, B. He, F. Zhang, H. Li, Peach gum for efficient removal of methylene blue and methyl violet dyes from aqueous solution, *Carbohydr. Polym.* 101 (2014) 574–581.
- [34] G. Annadurai, R. Juang, D. Lee, Use of cellulose based wastes for adsorption of dyes from aqueous solutions, *J. Hazard. Mater.*, 92 (2002) 263–274.
- [35] R. Xu, S. Xiao, J. Yuan, A. Zhao, Adsorption of methyl violet from aqueous solutions by the biochars derived from crop residues, *Bioresour. Technol.*, 102 (2011) 10293–10298.
- [36] I.D. Mall, V.C. Srivastava, N.K. Agarwal, Removal of Orange-G and Methyl Violet dyes by adsorption onto bagasse fly ash – kinetic study and equilibrium isotherm analyses, *Dyes Pigm.*, 69 (2006) 210–223.
- [37] A. Machrouhi, M. Farnane, A. Elhalil, R. Elmoubarki, M. Abdennouri, S. Qourzal, H. Tounsadi, N. Barka, Effectiveness of beetroot seeds and H<sub>3</sub>PO<sub>4</sub> activated beetroot seeds for the removal of dyes from aqueous, *J. Water Reuse Desal.*, doi: 10.2166/wrd.2017.034.
- [38] S. Xua, J. Wang, R. Wu, J. Wang, H. Li, Adsorption behaviors of acid and basic dyes on cross linked amphoteric starch, *Chem. Eng. J.*, 117 (2006) 161–167.
- [39] B.H. Hameed, Equilibrium and kinetic studies of methyl violet sorption by agricultural waste, *J. Hazard. Mater.*, 154 (2008) 204–212.
- [40] Y.S. Ho, W.T. Chiu, C.C. Wang, Regression analysis for the sorption isotherms of basic dyes on sugarcane dust, *Bioresour. Technol.*, 96 (2005) 1285–1291.
- [41] L.B.L. Lim, N. Priyantha, C. Hei Ing, M. Khairud Dahri, D.T.B. Tennakoon, T. Zehra, M. Suklueng, *Artocarpus odoratissimus* skin as a potential low-cost biosorbent for the removal of methylene blue and methyl violet 2B, *Desal. Wat. Treat.*, 53 (2015) 964–975.
- [42] M.K. Dahri, M.R.R. Kooh, L.B.L. Lim, Application of *Casuarina equisetifolia* needle for the removal of methylene blue and malachite green dyes from aqueous solution, *Alexandria Eng. J.*, 54 (2015) 1253–1263.
- [43] B.H. Hameed, A.A. Ahmad, Batch adsorption of methylene blue from aqueous solution by garlic peel, an agricultural waste biomass, *J. Hazard. Mater.*, 164 (2009) 870–875.
- [44] E.-K. Guechi, O. Hamdaoui, Sorption of malachite green from aqueous solution by potato peel: kinetics and equilibrium modeling using non-linear analysis method, *Arabian J. Chem.*, 9 (2016) S416–S424.
- [45] S. Hosseini, M.A. Khan, M.R. Malekbala, W. Cheah, T.S.Y. Choong, Carbon coated monolith, a mesoporous material for the removal of methyl orange from aqueous phase: adsorption and desorption studies, *Chem. Eng. J.*, 171 (2011) 1124.